

Dielectric Relaxation Properties in Polypropylene–Polyurethane Composites

G. BÁNHEGYI* and F. E. KARASZ, *Polymer Science and Engineering Department, University of Massachusetts, Amherst, Massachusetts 01003*, and Z. S. PETROVIĆ, *Institute for Petrochemistry, Gas, Oil and Chemical Engineering, Faculty of Technology, Novi Sad, Yugoslavia*

Synopsis

AC dielectric relaxation properties of polypropylene/polyurethane composites have been studied. The segmented polyurethane (PUR) component contained a poly(propylene oxide) soft segment, and a diphenyl methane diisocyanate/butanediol hard segment. The molecular weight of the soft segment, the concentration of the latter in the polyurethane phase, and the PUR content of the blends were changed systematically. It was observed that the polypropylene is phase-separated with respect to both PUR segments and that the dielectric relaxation properties are determined largely by the PUR component. Two transitions attributable to the glass transitions of the soft and hard phases, respectively, were observed. The soft segment transition temperature decreases with increasing molecular weight of the latter. The transition temperatures are somewhat dependent on the PUR content in the blend, indicating some interaction between the phases. Model calculations show that these shifts and some intensity anomalies are not due simply to the existence of a heterogeneous structure. The ohmic interfacial relaxation process does not play an important role in the temperature and frequency range studied.

INTRODUCTION

The relaxation properties of polymer blends have received attention in part because these properties can reveal details of the phase structure of these systems and provide information about interactions between blend constituents.¹⁻³

Blends of polypropylene (PP) with elastomeric materials are important because blending improves the impact resistance of polypropylene at low temperatures (see, for example, Refs. 4 and 5). Such blends are usually immiscible two phase systems. Immiscibility has been observed even with the chemically similar EPDM rubbers, so immiscibility with the structurally different polyurethanes (PUR) investigated in this contribution is anticipated.

Morphological, thermal, and mechanical (DMA, tensile, impact) properties of certain PP/PUR systems have been studied recently.⁶ The main conclusions can be summarized as follows:

1. Electron microscopic studies show that the PUR phase forms well-dispersed globular inclusions in the PP phase at low volume concentrations, while, around 30 wt % or above, agglomeration and the formation of

* Present address: Biopharm, Ltd. Research and Development, H-1087, Budapest, Hungary.

elongated rodlike particles begins and the PUR phase gradually achieves continuity.

2. WAXS studies show that the crystallinity of the PP phase decreases slightly with increasing PUR content (from about 65 to 55 wt %).
3. DSC studies could not detect the T_g of the PUR component but have shown that the melting temperature of PP remained essentially constant (167°C).
4. The addition of PUR did not change the location of the β -relaxation peak of PP, as detected by DMA (i.e., 24°C).

In this contribution we present some additional data on these systems. Dielectric spectroscopy can be regarded as a method complementary to dynamic mechanical analysis.^{7,8} In principle, the same molecular motions are detected by both methods, but the electrical field excites only polar species, so that dielectric spectroscopy has an aspect of selectivity. Dielectric spectroscopy is therefore an ideal tool for studying the systems discussed here since a polar minority phase is dispersed in an apolar matrix, and, as will be shown, the transitions in the polar phase which are more or less undetectable in DSC or DMA measurements appear clearly in the analyses of the dielectric properties.

EXPERIMENTAL

The polyurethane components of the blends were synthesized from poly(propylene oxide) (PPO) (Soda-So Co., Yugoslavia), forming the soft segment and diphenyl methane diisocyanate (MDI) as the hard segment; the chain extender was butanediol (BD). Two different polypropylene glycols were used ($M_w = 1000$ and 2000 , respectively), providing 1 degree of freedom. In addition, the concentration of the soft segment (SSC, %) was also varied between 50 and 70 wt %. The compositions of the samples and the codes used are given in Table I. The polypropylene component in all cases was Hipolen MA3 (Hipol, Odzaci, Yugoslavia) with MFI = 11. Blends were prepared in a Haake Rheomix type mixer at 45 rpm with a mixing time of 5 min at 180°C. Samples, 0.5 mm thick, were molded at 230°C for 2 min at low pressure followed by exposure to 70 atm at the same temperature for 2 min and were then cooled and held at 120°C for 2 min.

Dielectric measurements were performed using a Polymer Laboratories dielectric thermal analyzer (DETA), which consists of a General Radio 1689M automatic digital RLC bridge, a thermostatable measuring cell with a temperature programming unit, and a Hewlett-Packard 9816 minicomputer with peripheral units (floppy disc drive, plotter, printer). The software was also supplied by Polymer Laboratories.

The samples were measured in the temperature scan mode at a 5°C/min heating rate under a prepurified N₂ atmosphere from -100 to 140°C. The samples softened at the highest temperatures. The electrode diameter was 33 mm, the samples were equipped with Al foil electrodes, and the interelectrode distance was adjusted with a screw. Thus the change in the empty capacitance was limited to the thermal dilatation of the ceramic units fixing the cell; this ca-

TABLE I
Notations and Compositions of the Samples

Series	\bar{M}_w of PPG	Soft segment cc (SSC %)	PUR content of the blends (wt %)
I	1000	50	5, 10, 15, 20
II	1000	60	5, 10, 15, 20, 30
III	2000	50	5, 10, 15, 20
IV	2000	60	5, 10, 15
V	2000	70	5, 10, 15, 20, 30, 40

capacitance change is much lower than that of the sample. The temperature dependence of the empty capacitance is not taken into account by the software used. With the present two-electrode cell design without a guard ring, losses below 10^{-3} cannot be detected with certainty.

RESULTS

The dielectric properties of pure polypropylene are relatively insensitive to change between -100 and 150°C . The permittivity (around 2.3 at room temperature) decreases somewhat with increasing temperature; the loss is usually very low (around 10^{-3}) and displays two small maxima, around 30 and 120°C at 1 kHz. The peak amplitude depends on crystallinity, oxidation, and the presence of impurities and additives.⁷⁻¹¹ The lower temperature relaxation is associated with the glass transition of the amorphous phase while the higher temperature peak is attributed to a crystalline transition.

In the blend samples, steplike changes in ϵ' and maxima in ϵ'' were observed in all cases and these changes were greater than those observed for pure PP. Figures 1 and 2 show the temperature dependent dielectric dispersion (ϵ') and loss (ϵ'') curves respectively for sample II/20 at five different frequencies. The presence of two transitions is clearly visible. The lower temperature transition is not well resolved in the lower frequency curves (at 20 and 100 Hz) because of the experimental sensitivity. The maxima for the higher temperature transition are above the measured temperature range at 10 and 100 kHz. The temperature dependent data are shown in a complex plane (Cole-Cole) plot (Fig. 3), and it can be seen that in the case of the low temperature transition the points taken at different frequencies lie practically on the same curve, but the higher temperature transition is thermorheologically complex, and the differing temperature data cannot be superposed by a simple $\log \nu$ shift. This can also be seen from the increasing amplitudes of the loss peaks with increasing frequency.

To compare the various sample series below, the following data have been selected: the 1 kHz loss curves (since they display both transitions), and the 100 Hz dispersion curves, because they show the maximum observable static permittivity value at the highest temperatures. Figures 4 and 5 show the 1 kHz loss maxima (ϵ'' max) and the 100 Hz permittivity values measured at 125°C

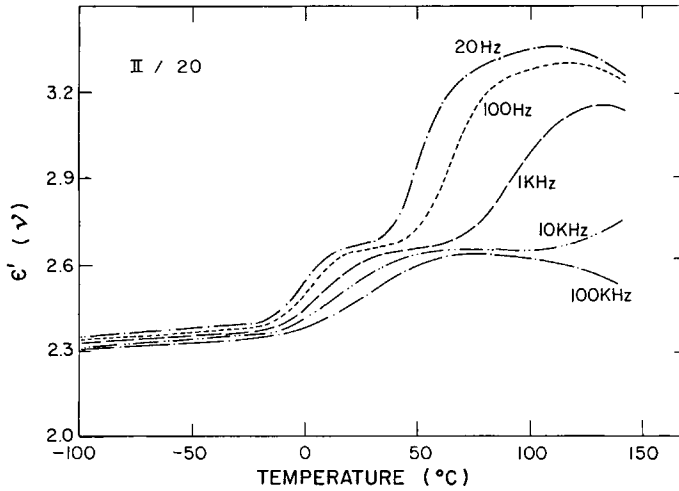


Fig. 1. Dielectric dispersion (ϵ') curves of a PP/PUR sample of series II containing 20 wt % polyurethane, measured at five different frequencies.

(above the higher transition temperature). In Figure 4 the loss maxima are plotted on a different scale because of the large intensity difference. The losses and static permittivities usually increase with increasing PUR concentration, but the increase is neither linear nor monotonic in all cases. The relaxation temperatures measured at different frequencies are presented for series I and II in Figure 6 (M_w of the soft segment is 1000) and for series III, IV, and V in Figure 7 (M_w of the soft segment is 2000). It is immediately apparent that the transition temperatures of the lower temperature transition are lower for series

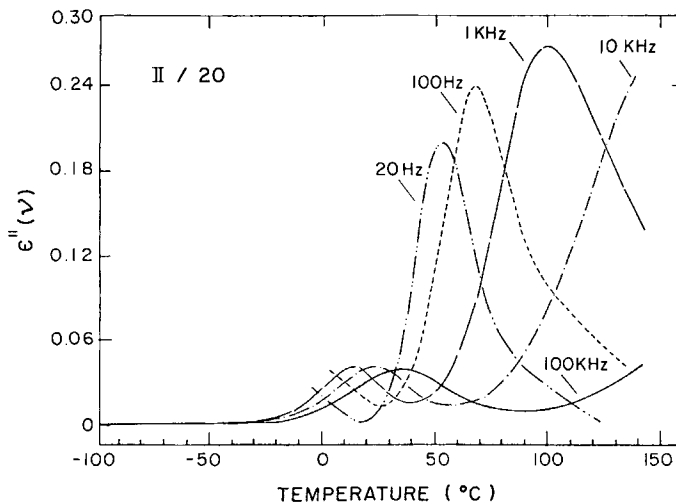


Fig. 2. Dielectric loss (ϵ'') curves of the sample shown in Figure 1 measured at five different frequencies.

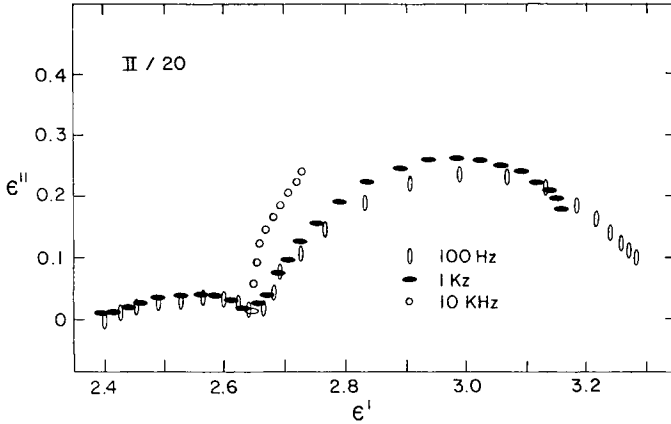


Fig. 3. Cole-Cole representation of the temperature-dependent dielectric dispersion and loss curves of sample II/20 measured at different frequencies.

III, IV, and V than for series I and II. The behavior of the high temperature transition is more complicated. It is also clear that the transition temperatures as a function of PUR content show some scatter; at best only trends can be established.

To compare the shapes of the relaxation curves, the 1 kHz data of the samples containing 10 wt % PUR are shown in Figure 8 in the Cole-Cole representation. One can see that the lower temperature relaxation process exhibits a wider

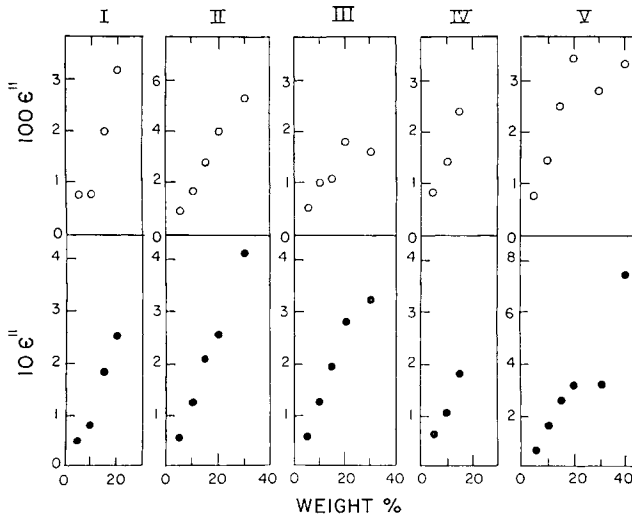


Fig. 4. Measured 1 kHz loss peak maxima as a function of polyurethane content in different series: (O) low temperature (soft segment) transition; (●) high temperature (hard segment) transition.

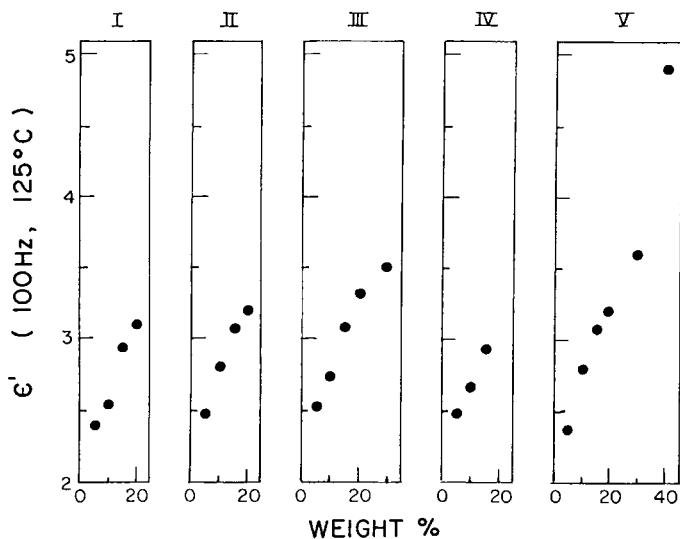


Fig. 5. Measured 100 Hz permittivities above the glass transition of the hard segment (usually at 125°C) as a function of the PUR content in the different series.

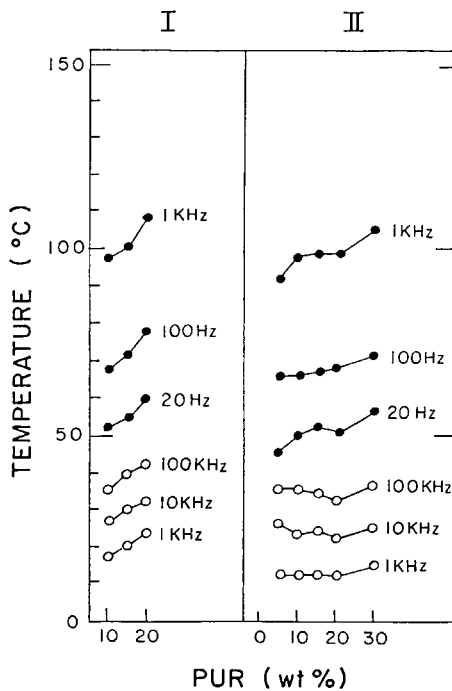


Fig. 6. Transition temperatures of samples of series I and II measured at different frequencies, plotted as a function of composition: (○) low temperature transition; (●) high temperature transition. The lines are not interpolation curves; they show only the connectivity of the data points.

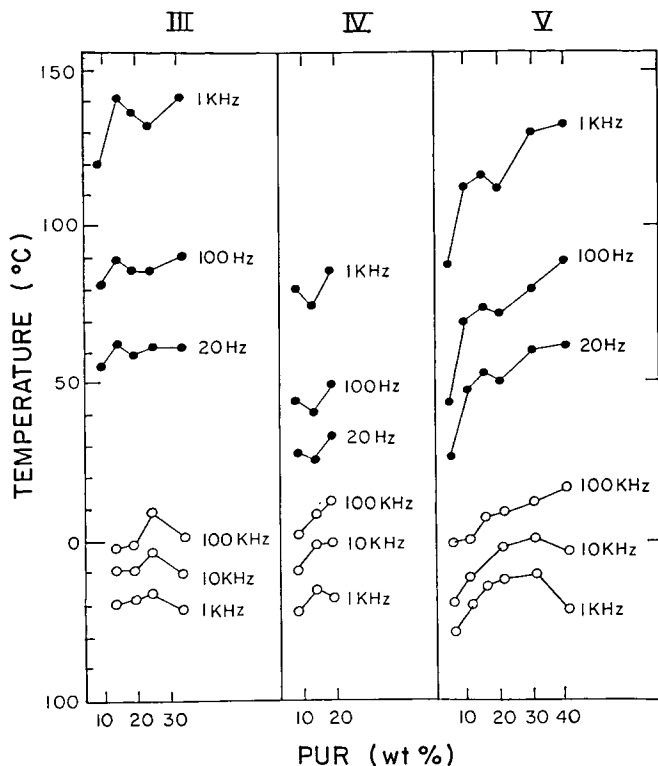


Fig. 7. Transition temperatures of samples of series III-V measured at different frequencies, plotted as a function of composition. Symbols are the same as in Figure 6.

relaxation time distribution; the skewed arc is very wide and flat. The shape and magnitude of the relaxation, however, change less than those of the high temperature transition from one series to another.

DISCUSSION

By comparing the dispersion (ϵ') and loss (ϵ'') curves obtained for these blend systems with those reported for pure PP,¹⁰ it becomes clear that practically the whole loss and dispersion are due to the presence of the polar additive.

Segmented block polyurethanes are themselves complex phase-separated systems consisting of at least two and sometimes four phases.¹² The soft and hard segment blocks tend to undergo microphase separation whose completeness and the sharpness of the boundary between the soft and hard phases depends on the chemistry of the system and on the thermal and solvent history of the sample. Depending on the chain length and the relative amounts of hard and soft phases both phases can be amorphous or semicrystalline.

The effect of the soft segment concentration on the transition temperatures and other physical properties has been studied for example in a poly-(tetramethylene oxide)/MDI/BD system over a wide composition range.^{13,14}

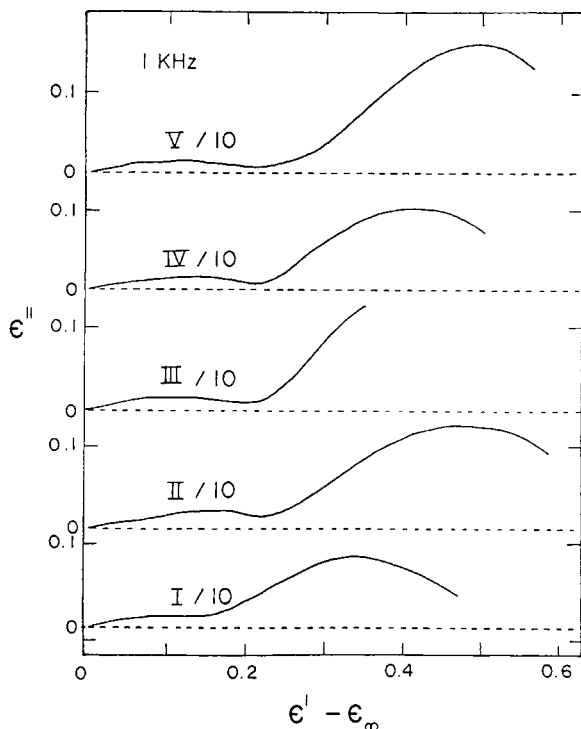


Fig. 8. Cole-Cole representation of the temperature-dependent 1-kHz data of composites containing 10 wt % PUR belonging to different series.

These references also contain information about earlier work in this field. The main conclusions regarding the specific transitions can be summarized as follows: The glass transition temperatures of the separated phases depend on the length of the blocks (determined by the weight average molecular weight of the soft phase and the soft segment concentration). The glass transition temperature of the soft phase decreases with increasing molecular weight, but remains higher than that of the soft segment homopolymer. This can be understood in terms of the looser network structure formed between the physical junctions of the hard phase. Crystallinity in the soft phase can be observed only at high molecular weights and high soft segment concentration, while the crystalline transition of the hard phase can be detected only at very low soft segment concentration. The T_g of the pure MDI/BD hard phase is 109°C ¹⁵; in segmented polyurethanes it usually drops to $80\text{--}90^\circ\text{C}$, depending on the concentration and crystallinity of the hard segment. The dilatometric T_g of the pure PPO polymer which constitutes the soft segment in our samples is -75°C .⁷ In AC dielectric measurements it shifts to about $-50\text{--}60^\circ\text{C}$ depending on the frequency used. Pure stereochemically regular PPO polymer is semicrystalline, but in our case no crystallinity is expected because of the atactic character of the PPO component.

Comparing these data with the transition temperatures observed in the PP/PUR composites (Figs. 6 and 7), one can see that the lower temperature transition, which can be attributed to the soft phase of the PUR component, de-

creases with increasing M_w of the soft segment, but it is still higher than the α transition temperature of the pure PPO phase, in accordance with the observations of Refs. 13 and 14. The dependence of transition temperatures on the soft segment concentration is not significant if the molecular weight of the soft segment is held constant. The transition temperatures shift, however, appreciably if the PUR content of the blend is varied. According to the thermal and dynamic mechanical measurements,⁶ the transitions of the PP component did not depend on the blend composition, and so the shift of the transitions of the PUR segments is probably due to morphological constraints or interfacial interactions in the phase-separated blends.

To interpret the absolute values of the losses and permittivities observed in the blends, the effect of the heterogeneous nature of these systems has to be investigated. Experimental evidence has shown that if two low loss materials such as polypropylene and polycarbonate (PC) are blended to form a phase-separated system,¹⁶ then the resulting permittivity will depend on the composition and the polarity difference of the components; the loss curve will be low and flat up to the glass transition temperature of, in this case, the PC component. If, however, the polarity and loss of the two components are widely different, as in the case of polyethylene and polyamide,¹⁷ at certain compositions the mixture can exhibit even higher permittivity and loss than either of the components, an effect related to the heterogeneous structure of the blend.

Model Calculations

To assess the possible effects of phase heterogeneity on the dielectric relaxation spectra in the present case, model calculations have been performed. The mixture formulae used to calculate the permittivity and other related properties of composites have been recently reviewed (see, e.g., Refs. 18 and 19). Model calculations have shown^{19,20} that matrix-inclusion type, effective medium and symmetric integral equations qualitatively predict different behaviors for the complex permittivities in the low frequency limit and for the conductivities of insulator-conductor composites. In this contribution we will use two relevant equations to simulate the dielectric response. First is the generalized Bruggeman equation for parallel oriented spheroids²¹:

$$\left(\frac{\bar{\epsilon} - \epsilon_2}{\epsilon_1 - \epsilon_2} \right) \left(\frac{\epsilon_1}{\bar{\epsilon}} \right)^A = 1 - v_2 \quad (1)$$

where $\bar{\epsilon}$ is the permittivity of the composite, ϵ_1 is that of the matrix phase (medium), ϵ_2 is that of the included phase, v_2 is the volume fraction of the inclusions, and A is the depolarization factor of the spheroid along that axis which is parallel to the electrical field (it is assumed that the field is directed along one of the axes). The depolarization factor can be calculated from the axial ratio (γ) of the inclusion (see, e.g., Ref. 19).

The other equation is the generalized Böttcher equation²²:

$$\frac{(\epsilon_1 - \bar{\epsilon})v_1}{\bar{\epsilon} + (\epsilon_1 - \bar{\epsilon})A} + \frac{(\epsilon_2 - \bar{\epsilon})v_2}{\bar{\epsilon} + (\epsilon_2 - \bar{\epsilon})A} = 0 \quad (2)$$

derived for a statistical mixture of parallel spheroidal particles, notation as above, $v_1 = 1 - v_2$. This equation is symmetric in indices; there is no *a priori* reason to assign any of the phases as matrix or inclusion. Calculations show that, for this equation in the $0 < v_2 < A$ range, phase 1 can be regarded as continuous and phase 2 as discrete; in the $A < v_2 < 1 - A$ region both phases are continuous while in the $1 - A < v_2 < 1$ range phase 2 is continuous and phase 1 is discrete.

In both cases ϵ can be real (ideal dielectrics) or complex (lossy dielectrics). In the latter case ϵ_k^* of the k th component is

$$\epsilon_k^* = \epsilon'_k - j(\epsilon''_k + \sigma_k/\epsilon_0\omega) \quad (3)$$

where ϵ'_k is the real part of the complex permittivity, ϵ''_k is the dielectric loss, σ_k is the ohmic conductivity, ϵ_0 is the vacuum permittivity, $\omega = 2\pi\nu$ is the radial frequency, ν is the frequency, and j is $\sqrt{-1}$.

The Effect of Inclusion Shape and Permittivity on the Permittivity of the Composite

First we consider the effect of the inclusion permittivity on that of the composite. Figure 9 shows this function at different volume fractions for globular

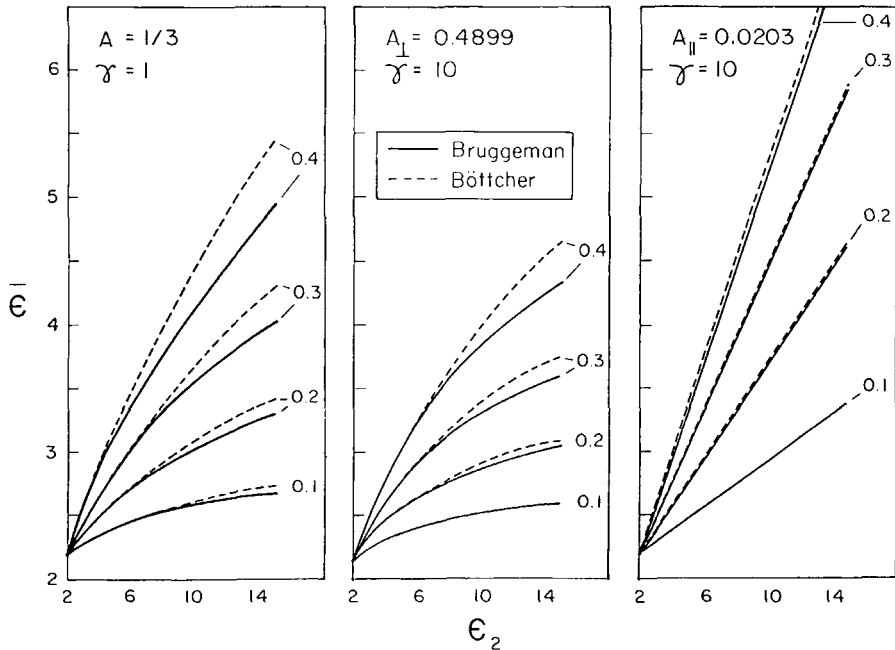


Fig. 9. Dielectric permittivity of a composite consisting of phase 1 with $\epsilon_1 = 2.2$ and phase 2 having varying permittivity at different volume fractions of the second phase. Left: spherical geometry ($\gamma = 1$). Center: elongated spheroidal geometry ($\gamma = 10$), perpendicular to the axis of rotation. Right: elongated spheroidal geometry ($\gamma = 10$), parallel with the axis of rotation. Depolarization factor values are given on the figures.

(left) and prolate (elongated) spheroids perpendicular (middle) and parallel (right) to the axis of rotation. It should be noted that the volume fractions are somewhat lower than the weight fractions, since the density of polypropylene ($\rho_1 = 0.90$) is lower than the typical value for polyurethanes ($\rho_2 = 1.1-1.2$), but this does not influence our general conclusions. With the exception of spheroids, field parallel with the axis of rotation, all functions deviate considerably from the linear, which implies that the increasing permittivity of the inclusions causes less and less increase in the permittivity of the composite. Elongated particles with an axial ratio of 10 are taken into account because, according to the morphological studies⁶ at higher volume fractions, the PUR globules tend to agglomerate and form elongated particles. If the orientation of the elongated particles is random, other formulae are appropriate (see Ref. 19), but as a first approximation the permittivity of the composite containing randomly oriented spheroids can be obtained as a 1:2 average of the parallel and perpendicular orientation values. The Bruggeman formula tends to predict a lower composite permittivity at a given level of inclusion permittivity. Comparing these theoretical values plotted in Figure 9 with the highest ϵ' values measured at 100 Hz (see Fig. 5), one can conclude that the static permittivity of the inclusions varies between 8 and 15, which is comparable to values observed for other polyurethanes (see, e.g., Refs. 23-26).

The Effect of Heterogeneity on the Position and Intensity of Loss Peaks

The effect of phase heterogeneity on the dielectric loss was modeled using the following simple dielectric function for the inclusion:

$$\epsilon^*(\nu, T) = \epsilon_\infty + \frac{\Delta\epsilon}{1 + j\{(\nu/\nu_0)\exp[(E_d/R)(1/T - 1/T_0)]\}} + \frac{\sigma_0 \exp(-E_c/RT)}{j\epsilon_0 2\pi\nu} \quad (4)$$

which is a Debye response⁸ with thermal activation. Here ϵ_∞ is the high frequency limiting permittivity, $\Delta\epsilon$ is the relaxation strength, T_0 is the maximum temperature measured at a frequency of ν_0 , ν is the actual frequency, R is the universal gas constant, E_d is the activation energy of relaxation, E_c is that of the conductivity, and σ_0 is the preexponential factor of the ohmic conductivity. In the model system $\epsilon_\infty = 2.5$, $\Delta\epsilon = 5$, $E_d = 100$ kJ/mol, $\nu_0 = 10^3$ Hz, and $T_0 = 80^\circ\text{C}$ have been chosen for phase 2. The calculated permittivity and loss are shown in Figure 10 as a function of temperature. In the case of the loss, the pure dielectric loss (curve a) and three other curves are shown at different conductivity levels. It is assumed that the room temperature conductivity is $10^{-11} \Omega^{-1} \text{cm}^{-1}$ in all cases and E_c is varied as 25, 50, and 75 kJ/mol in curves b, c, and d, respectively. Using these values for the inclusion and, for the sake of simplicity, $\epsilon' = 2.2$ and $\epsilon'' = 10^{-3}$, independent of temperature, for the matrix, various properties of the model composite have been calculated and these trends compared to the experimental values.

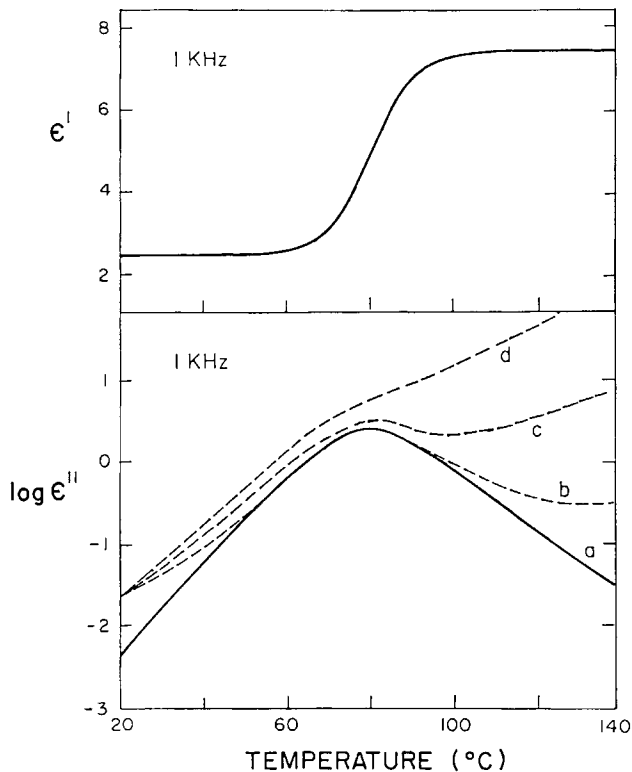


Fig. 10. Dielectric dispersion and loss of a system described by eq. (4) setting $\epsilon_{\infty} = 2.5$, $\Delta\epsilon = 5$, $\nu_0 = 10^3$ Hz, $\nu = 10^3$ Hz, $T_0 = 80^\circ\text{C}$, $E_d = 100$ kJ/mol. The ohmic conduction is neglected in curve a ($\sigma_0 = 0$), while $\sigma(20^\circ\text{C}) = 10^{-11} \Omega^{-1} \text{cm}^{-1}$ is assumed with $E_c = 25, 50,$ and 75 kJ/mol in curves b, c, and d, respectively. ϵ' is independent of the conductivity level.

The effect of phase heterogeneity on the loss peak height of the second component in the absence of ohmic conduction (ϵ'' is approximated by curve a of Fig. 10) is first examined. Figure 11 shows the ratio of the composite loss peak height to that of pure second component for spherical (left) and for elongated spheroidal (right) inclusions. In the latter case both parallel and perpendicular orientations were calculated; the 1 : 2 average is also shown as a first approximation for the random orientation. The losses are in all cases lower than would be expected from the linear mixing rule, but they increase monotonically with the concentration of the second phase. Values obtained for spheres and for randomly oriented spheroids are very close to each other, so that intensity anomalies (see Fig. 4) obtained experimentally (e.g., in series V at 30 wt % PUR) cannot be simply explained by switching from a globular to a fibrillar morphology.

The effect of phase heterogeneity on the loss peak temperatures has been assessed using $\epsilon'_1 = 2.2$ and $\epsilon''_1 = 10^{-3}$ for the matrix and curve a of Figure 10 for the inclusion. Calculating the temperature dependent loss peaks for the composites in the $\nu_2 = 0.1-0.4$ concentration range, it is observed that T_{max} of the loss peak shifts from 80 to 75–78°C. The experimentally observed shifts exceed 3–5°C (see Figs. 5 and 6), which can be explained only if we assume

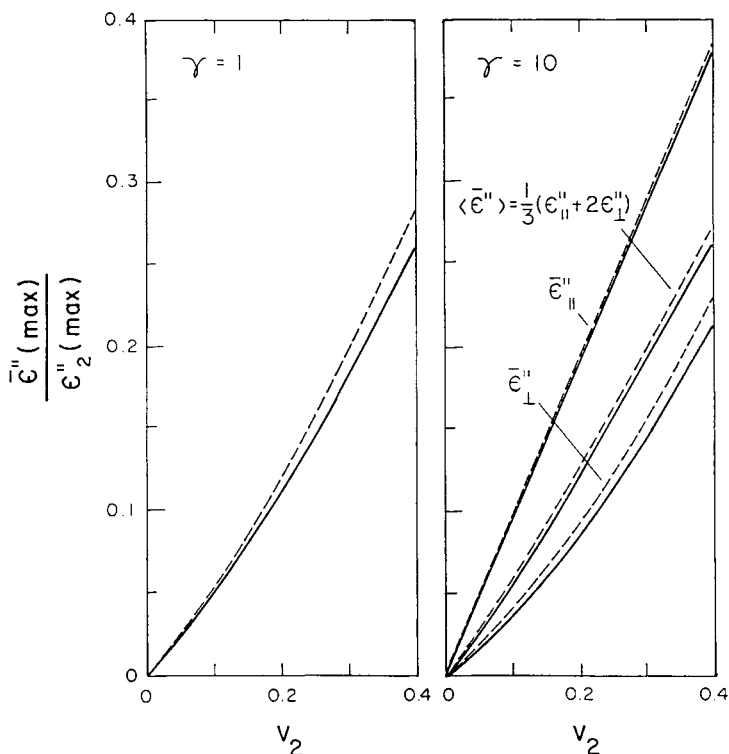


Fig. 11. Relative height of the loss maxima in a composite consisting of phase 1 with $\epsilon'_1 = 2.2$, $\epsilon''_1 = 10^{-3}$, and phase 2 described by curve a in Figure 10, as a function of the concentration of the second phase for spherical (left) and elongated spheroidal (right, $\gamma = 10$) geometries. In the latter case, the directions parallel and perpendicular to the axis of rotation are also given together with their 1 : 2 average, which is a first estimate for the random orientation.

that the transition properties of the PUR phase depend on the blend compositions, probably because of morphological changes.

Similarly the apparent frequency dependence of the peak intensity of the hard segment transition demonstrated in Figure 2 (which leads to the breakdown of the time-temperature superposition shown in Fig. 3) can be understood only if we assume that the relaxation strength of the hard segment transition depends on the temperature. This is an intrinsic property of the PUR phase and can be understood assuming that the number or steric correlation of mobile dipoles changes with temperature (see, e.g., Refs. 8, 26, and 27) simultaneously with the gradual breaking up of intermolecular H bonds.

Possible Effect of Interfacial Polarization

Finally we have examined the combined effect of dielectric and ohmic loss on the dielectric behavior in our model system. Permittivities and losses calculated by the Bruggeman and Böttcher equations are shown in Figures 12 and 13, respectively. Room temperature conductivity of the inclusion phase is $10^{-11} \Omega^{-1} \text{ cm}^{-1}$ in all cases, E_c is 25, 50, and 75 kJ/mol for curves a, b, and c, respectively (according to curves b, c, and d in Fig. 10, respectively). In the case

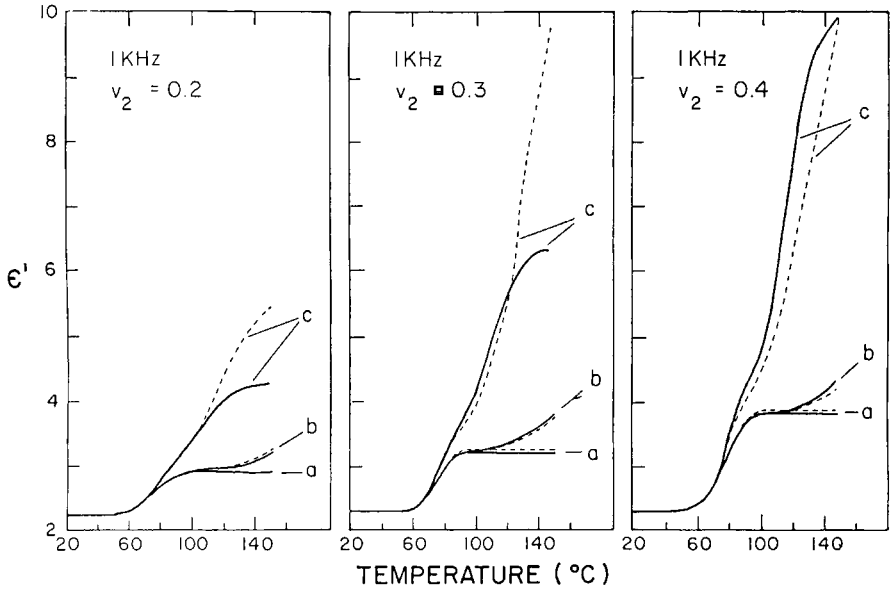


Fig. 12. 1 kHz permittivity curves of systems consisting of phase 1 with $\epsilon'_1 = 2.2$, $\epsilon''_1 = 10^{-3}$ and phase 2 described by curves b, c, and d in Figure 10 (curves a, b, and c in this figure, respectively) at different concentrations of the second phase. The dashed lines denote the Böttcher equation, the solid line shows the Bruggeman equation. $A = \frac{1}{3}$ is used in all cases.

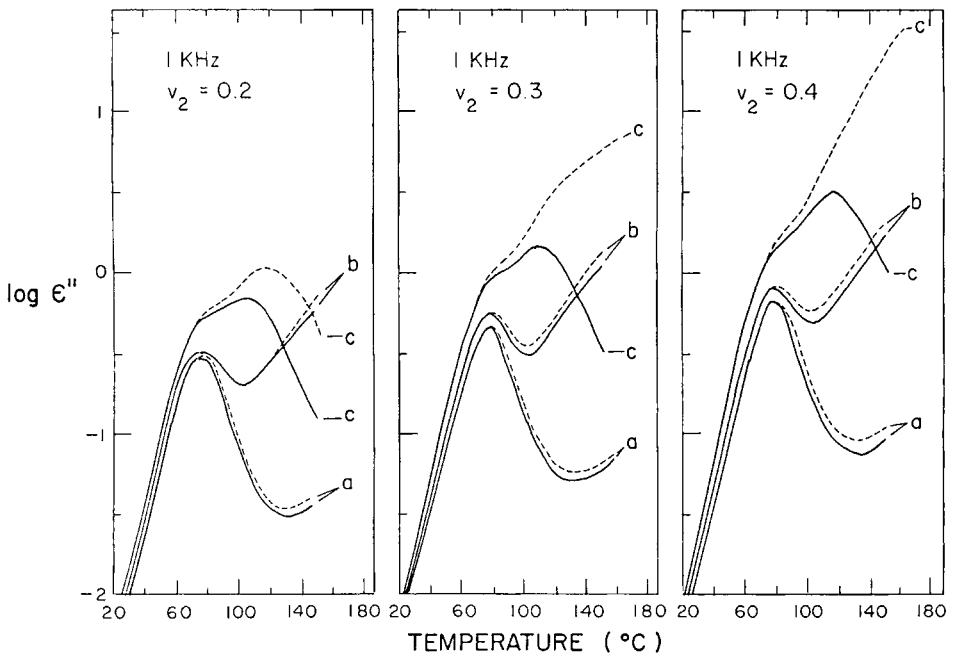


Fig. 13. Loss curves of the systems given in Figure 12.

of $E_c = 25$ kJ/mol (curve a) the dielectric loss of the inclusion is dominant; there is no sign of an ohmic interfacial relaxation process. In case b, (the $E_c = 50$ kJ/mol) the effect of ohmic loss becomes significant at the highest temperatures, and the dielectric permittivity begins to increase again, indicating the onset of the ohmic interfacial or Maxwell-Wagner relaxation. In case c ($E_c = 75$ kJ/mol) the dielectric loss peak cannot be distinguished from that of the interfacial relaxation process. In the last case the qualitative difference between the Böttcher and Bruggeman equations is quite evident. Although the Bruggeman equation predicts a decreasing loss after the interfacial loss peak at all three volume fractions studied, the Böttcher equation predicts an increasing ohmic loss above $v_2 = \frac{1}{3}$ for spherical inclusions due to the percolation of the more conductive second phase.

Permittivities exceeding 4 have been observed experimentally only in series V at the highest soft segment concentration (see Fig. 5); thus it is certain that the ohmic interfacial process does not play an important role in the frequency and temperature range studied. From this fact it follows that either the room temperature conductivity of the PUR components is much lower than $10^{-11} \Omega^{-1} \text{ cm}^{-1}$ or their activation energies are low, in the order of 20–30 kJ/mol. Interfacial losses are expected to appear first on the lowest frequency curves; therefore the 20 Hz loss curves of some series are shown in Figures 14–16. A high temperature shoulder and occasionally the beginning of the conductivity tail can be observed at the highest temperatures, but the magnitude of this “side process” is much less than that of the expected ohmic interfacial relaxation process. The onset of conductivity at the highest frequencies is probably related to the morphological changes of the PUR phase; the elongation of the particles decreases the percolation threshold.

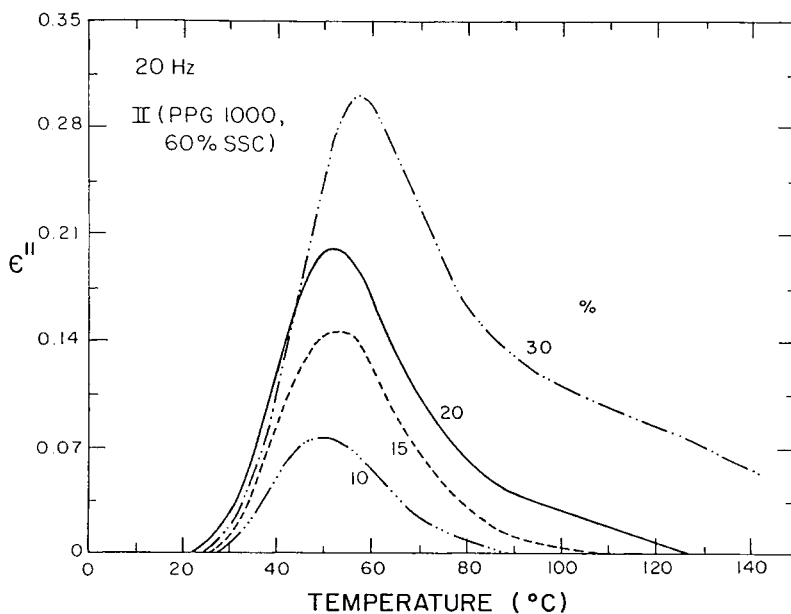


Fig. 14. Loss curves of samples of series II measured at 20 Hz.

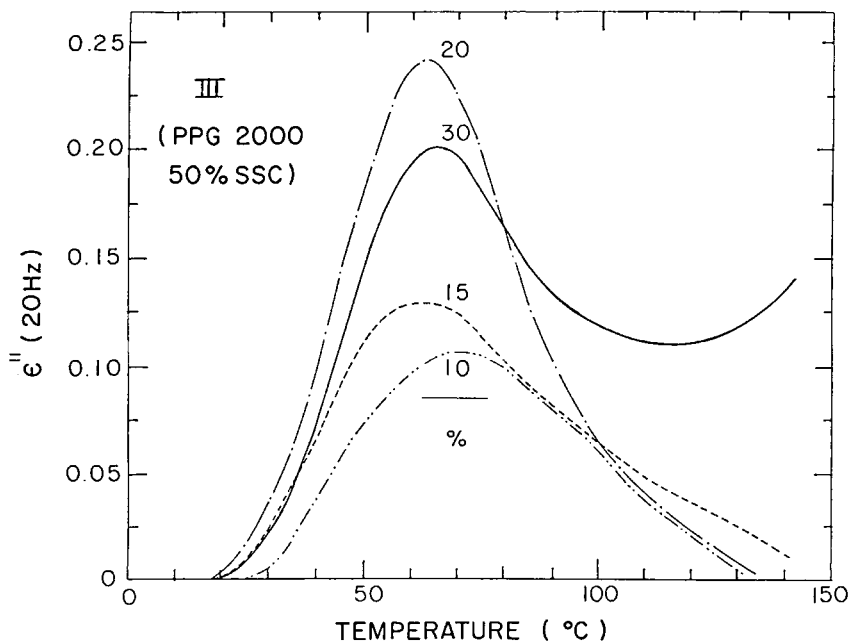


Fig. 15. Loss curves of samples of series III measured at 20 Hz.

CONCLUSIONS

The dielectric relaxation behavior of some polypropylene/polyurethane blends has been investigated and the main findings can be summarized as follows:

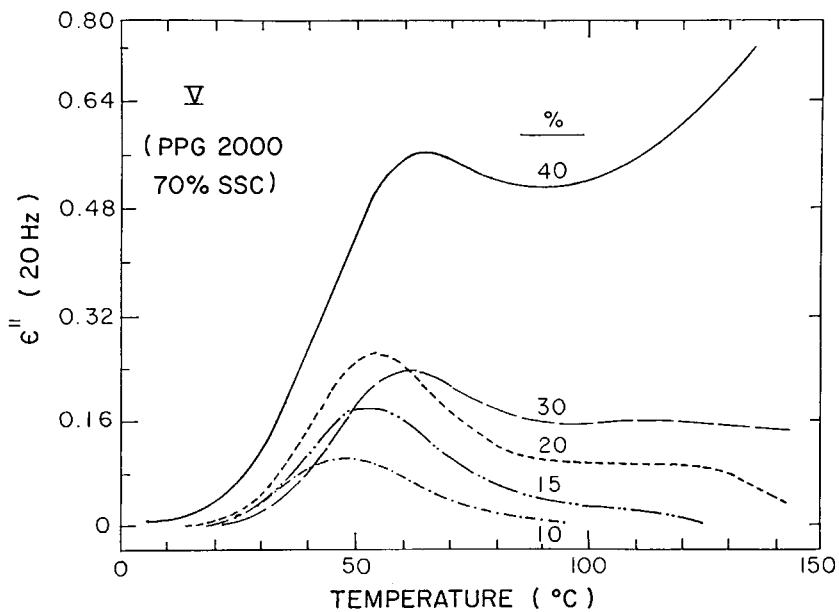


Fig. 16. Loss curves of samples of series V measured at 20 Hz.

1. In agreement with earlier investigations,⁶ the system was shown to be phase-separated. The transition temperatures of the polyurethane phase in some cases showed a concentration dependence, indicating the presence of some kind of interaction at the supermolecular level.
2. The soft segment transition temperature decreased with increasing molecular weight of the soft segment. The soft segment transition temperature was not strongly dependent on the soft segment concentration at a given molecular weight of the soft segment. The hard segment transition temperatures passed through a minimum as a function of the soft segment concentration if the molecular weight of the soft segment was 2000. However, we used only three soft segment concentrations (50, 60, and 70%); thus this behavior cannot be explained on the basis of these experiments only.
3. The soft segment transitions showed a wider relaxation time distribution (flat and wide Cole-Cole plot) than the hard segment transitions. The soft segment transition varied less from composite to composite if the PUR component was held constant than the hard segment transition. The Cole-Cole curves of the soft segment transition measured at different frequencies as a function of the temperature could be described by practically the same function, while hard segment transition proved to be thermorheologically complex.
4. The loss maxima tended to increase with increasing PUR concentration with a few exceptions. The lowest frequency (20 Hz) loss data showed that at the highest temperatures (above the hard segment transition) either there was another transition of low intensity or the hard segment transition was doubled. At higher PUR contents, where the PUR particles tended to form aggregates or elongated particles, the conductivity tail of the PUR component appeared as a consequence of the percolation phenomenon.
5. Model calculations were used to estimate the possible effect of phase heterogeneity on the observed properties. It was observed that: Phase heterogeneity can cause a shift of the transition temperatures of a few degrees in the negative direction, but it cannot explain the 10–20°C shifts observed experimentally; phase heterogeneity and changes in morphology are not responsible for relaxation intensity concentration anomalies observed in some cases and for the thermorheologically complex behavior of the hard segment transition in the composites; there is no sign of the ohmic interfacial relaxation process in the temperature and frequency range studied.

One of us (F.E.K.) acknowledges AFOSR Grant 88-001 for support.

References

1. J. A. Manson and L. H. Sperling, *Polymer Blends and Composites*, Plenum, New York, 1976.
2. D. R. Paul and S. Newman (Eds.), *Polymer Blends*, Academic, New York, 1978.
3. E. Martuscelli, R. Palumbo, and M. Kryszewski (Eds.), *Polymer Blends, Processing, Morphology and Properties*, Plenum, New York, 1980.

4. J. Karger-Kocsis, A. Kalló, and G. Bodor, *Gummi Asbest Kunststoffe*, **36**, 101 (1983).
5. J. Karger-Kocsis, Z. Balajthy, and L. Kollár, *Kunststoffe*, **74**, 104 (1984).
6. Z. Petrović, J. Budinski-Simendić, A. Nemes, and V. Divjaković, in *Proceedings of the European Technical Conference, "Eurotech 88" on Polypropylene*, Paris, 1988, p. 7.
7. N. G. McCrum, B. E. Read, and G. Williams, *Anelastic and Dielectric Effects in Polymeric Solids*, Wiley, London, 1967.
8. P. Hedvig, *Dielectric Spectroscopy of Polymers*, Adam Hilger, Bristol, 1977.
9. E. O. Forster, 1973 Ann. Rep. CEIDP, National Academy of Sciences, Washington, DC, 1974, p. 447-455.
10. H. Kramer and K. E. Helf, *Kolloid Z.*, **180**, 114 (1962).
11. T. Umemura, T. Suzuki, and T. Kashiwazaki, *IEEE Trans. Electr. Insul.*, **EI-17**, 300 (1982).
12. Y. Y. Kercha, *Physical Chemistry of Polyurethanes* (in Russian), Naukova Dumka, Kiev, 1979.
13. Z. S. Petrović and J. Budinski-Simedić, *Rubber Chem. Technol.*, **58**, 685 (1985).
14. Z. S. Petrović and J. Budinski-Simedić, *Rubber Chem. Technol.*, **58**, 701 (1985).
15. C. Hepburn, *Polyurethane Elastomers*, Elsevier, Amsterdam, 1982.
16. P. K. C. Pillai, G. K. Narula, and A. K. Tripathi, *Polym. J.*, **16**, 575 (1984).
17. F. P. LaMantia, A. Valenza, and D. Acierno, *Coll. Polym. Sci.*, **263**, 726 (1985).
18. R. L. McCullough, *Compos. Sci. Technol.*, **22**, 3 (1985).
19. G. Bánhegyi, *Coll. Polym. Sci.*, **264**, 1030 (1986).
20. G. Bánhegyi, *Coll. Polym. Sci.*, **266**, 11 (1988).
21. M. H. Boyle, *Coll. Polym. Sci.*, **263**, 51 (1985).
22. W. Y. Hsu, T. D. Gierke, and D. J. Molnar, *Macromolecules*, **16**, 1945 (1983).
23. A. M. North, J. C. Reid, and J. B. Shortall, *Eur. Polym. J.*, **5**, 565 (1969).
24. A. M. North and J. C. Reid, *Polym. J.*, **8**, 1129 (1972).
25. S. B. Dev, A. M. North, and J. C. Reid, in *Dielectric Properties of Polymers*, F. E. Karasz, Ed., Plenum, New York, 1972, p. 217.
26. G. Bánhegyi, M. K. Rho, J. C. W. Chien, and F. E. Karasz, *J. Polym. Sci., Polym. Phys. Ed.*, **25**, 57 (1987).
27. G. Bánhegyi, P. Hedvig, and F. E. Karasz, *J. Appl. Polym. Sci.*, **35**, 679 (1988).

Received February 13, 1989

Accepted March 20, 1989